Chemistry of Metals and Alloys

Chem. Met. Alloys 6 (2013) 12-19
Ivan Franko National University of Lviv
www.chemetal-journal.org

On the formation of ternary phases in the Ti–Fe–Sn ternary system at 773 K

L. ROMAKA[1]*, V.V. ROMAKA[2], Yu. STADNYK[1], N. MELNYCHENKO[1,3]

[1] *Department of Inorganic Chemistry, Ivan Franko National University of Lviv,*
    Kyryla i Mefodiya St. 6, UA-79005 Lviv, Ukraine
[2] *Department of Materials Engineering and Applied Physics, Lviv Polytechnic National University,*
    Ustyyanovycha St. 5, UA-79013 Lviv, Ukraine
[3] *Army Academy named after Hetman Petro Sahaydachnyi,*
    Gvardiyska St. 32, UA-79012 Lviv, Ukraine
* *Corresponding author. E-mail: romakal@franko.lviv.ua*

The phase equilibria of the Ti–Fe–Sn ternary system were studied at 773 K in the whole concentration range using X-ray diffraction and metallographic analyses. The Ti–Fe–Sn ternary system at 773 K is characterized by the formation of three ternary intermetallic compounds: $TiFe_2Sn$ ($MnCu_2Al$-type), Ti_5FeSn_3 (Hf_5CuSn_3-type), and $Ti_{0.4}Fe_{0.6}Sn_2$ (Mg_2Ni-type). The existence of substitutional solid solutions $TiFe_{2-x}Sn_x$ (up to 5 at.% Sn) and $Ti_{6-x}Fe_xSn_5$ (up to 5 at.% Fe) was observed. The limiting composition of the $Ti_5Fe_xSn_3$ solid solution ($x = 1.0$) is considered as a distinct compound with Hf_5CuSn_3 structure type.

Stannides / Phase diagram / Solid solution / EPMA / Electronic structure

Introduction

In the course of scientific and technological progress, large attention is paid to the development of new functional materials based on intermetallic compounds. In search of new intermetallics having specific thermoelectric properties, we focus on the investigation of ternary systems with elements of group IVb, *d*-metals and Sn or Sb. Most of the studied systems are characterized by the presence of equiatomic compounds [1-6]. Among them, the *Me*NiSn stannides (*Me* = Ti, Zr, Hf), crystallizing with the cubic MgAgAs-type (half-Heusler phases), are prospective semiconducting materials for thermoelectric applications [7-11]. Changing the *d*-elements leads to different crystal structures for the *MeMe*'Sn stannides (ZrCoSn, HfCoSn – hexagonal ZrNiAl-type [1,2], ZrCuSn – orthorhombic TiNiSi-type [5], TiCuSn – hexagonal LiGaGe-type [12]) and results in a change of the semiconducting properties to metallic type of conductivity. In the case of the Ti–Mn–Sn and {Zr,Hf}–Ag–Sn systems, the absence of equiatomic compounds was noticed [13,14]. In some cases the formation of half-Heusler *MeMe*'Sn compounds is also very sensitive to the preparation method and heat treatment. For a proper understanding of these influences, a detailed knowledge of the phase relations in metallic systems is a prerequisite.

In this paper we present for the first time the results of X-ray and EPM analyses of the phase equilibria in the Ti–Fe–Sn ternary system at 773 K and an analysis of the formation of some of the ternary phases.

Experimental

The samples were prepared by direct arc melting of the constituent elements (titanium, 99.99 wt.% purity; iron, 99.99 wt.% purity; tin, 99.999 wt.% purity) under high-purity Ti-gettered argon atmosphere on a water-cooled copper crucible. The alloys were annealed at 773 K in evacuated quartz tubes for 720 h, and subsequently quenched in ice water.

X-ray phase analysis of the samples was carried out using powder patterns obtained on a DRON-4.0 (Fe *K*α radiation) diffractometer. The observed diffraction intensities were compared with reference powder patterns of binary and known ternary phases. The lattice parameters were refined by least-squares fits to indexed 2*θ*-values using the WinCSD program package [15].

The chemical compositions of the samples were examined by Scanning Electron Microscopy (SEM) using Zeiss Supra 55VP and REMMA-102-02 scanning electron microscopes. Quantitative electron probe microanalysis (EPMA) of the phases

Table 1 Crystallographic characteristics of the binary phases in the Ti–Fe, Fe–Sn and Ti–Sn systems at 773 K (this work).

Phase	Pearson symbol	Space group	Structure type	Lattice parameters, nm		
				a	*b*	*c*
TiFe$_2$	*hP*12	*P*6$_3$/*mmc*	MgZn$_2$	0.4772(1)	–	0.7796(2)
TiFe	*cP*2	*Pm-3m*	CsCl	0.29802(2)	–	–
FeSn	*hP*6	*P*6/*mmm*	CoSn	0.5287(3)	–	0.4427(5)
FeSn$_2$	*tI*12	*I*4/*mcm*	CuAl$_2$	0.6535(5)	–	0.5333(4)
Ti$_2$Sn$_3$	*oS*40	*Cmca*	Ti$_2$Sn$_3$	0.5910(2)	1.9837(8)	0.7055(3)
Ti$_6$Sn$_5$	*oI*44	*Immm*	Ti$_6$Sn$_5$	0.5662(6)	0.9060(4)	1.7059(5)
Ti$_5$Sn$_3$	*hP*16	*P*6$_3$/*mcm*	Mn$_5$Si$_3$	0.8047(3)	–	0.5455(3)
Ti$_2$Sn	*hP*6	*P*6$_3$/*mmc*	Ni$_2$In	0.4611(8)	–	0.5615(9)
Ti$_3$Sn	*hP*8	*P*6$_3$/*mmc*	Mg$_3$Cd	0.5875(6)	–	0.4750(5)

Table 2 Lattice parameters of the TiFe$_{2-x}$Sn$_x$ solid solution.

Composition	Lattice parameters, nm		*V*, nm^3
	a	*c*	
Ti$_{33}$Fe$_{67}$	0.4772(1)	0.7793(2)	0.1536(6)
Ti$_{33}$Fe$_{65}$Sn$_3$	0.4786(2)	0.7808(5)	0.1548(1)
Ti$_{33}$Fe$_{62}$Sn$_5$	0.4801(6)	0.7830(1)	0,1563(2)
Ti$_{33}$Fe$_{60}$Sn$_7$ [a]	0.4802(2)	0,7831(5)	0,1563(1)

[a] Two-phase sample.

Table 3 Lattice parameters of the Ti$_{6-x}$Fe$_x$Sn$_5$ solid solution.

Composition	Lattice parameters, nm		*V*, nm^3
	a	*c*	
Ti$_{55}$Sn$_{45}$	0.9205(8)	0.5709(5)	0.4189(6)
Ti$_{52}$Fe$_3$Sn$_{45}$	0.9199(5)	0.5704(6)	0.4180(5)
Ti$_{50}$Fe$_5$Sn$_{45}$	0.9201(3)	0.5684(5)	0.4167(4)
Ti$_{48}$Fe$_7$Sn$_{45}$ [a]	0.9196(2)	0.5681(5)	0.4160(3)

[a] Two-phase sample.

was carried out using an energy-dispersive X-ray analyzer with the pure elements as standards (the acceleration voltage was 20 kV; *K*- and *L*-lines were used).

DFT (Density Functional Theory) electronic structure calculations for one of the ternary compounds in the system (with experimentally determined structural parameters) were carried out with the Elk package [16] (an all-electron full-potential linearized augmented-plane wave code with PBE [17] parameterization). VESTA [18] was used for crystal structure and volumetric data visualization of the electron density and electron localization function (ELF).

Results and discussion

Isothermal section of the Ti–Fe–Sn system
The phase equilibria in the Ti–Fe–Sn system at 773 K were studied by means of X-ray diffraction and scanning electron microscopy of 10 binary and 52 ternary alloys (Fig. 1). As regards the boundary systems, all the binary compounds were confirmed and the corresponding crystallographic characteristics are reported in Table 1. An analysis of literature data concerning the Ti–Sn binary phase diagram [19] showed the presence of four binary compounds: Ti$_3$Sn, Ti$_2$Sn, Ti$_5$Sn$_3$ and Ti$_6$Sn$_5$. Additional information about the Ti$_2$Sn$_3$ compound with Ti$_2$Sn$_3$-type was reported in [20]. To check the existence of the Ti$_2$Sn$_3$ binary stannide under our conditions, a sample of composition Ti$_{40}$Sn$_{60}$ was prepared and annealed at 773 K. Phase analysis of the annealed Ti$_{40}$Sn$_{60}$ sample clearly showed the presence of the Ti$_2$Sn$_3$ compound with Ti$_2$Sn$_3$-type (Table 1) at the temperature of the investigation.

According to the phase analysis, formation of substitutional solid solutions TiFe$_{2-x}$Sn$_x$, based on binary TiFe$_2$ (MgZn$_2$-type), and Ti$_{6-x}$Fe$_x$Sn$_5$, based on binary Ti$_6$Sn$_5$ (Ti$_6$Sn$_5$-type), up to 5 at.% Sn and 5 at.% Fe, respectively, was observed (Tables 2 and 3).

Table 4 Crystallographic characteristics of the ternary compounds in the Ti–Fe–Sn system at 773 K.

No. [a]	Compound	Space group	Structure type	Lattice parameters, nm		
				a	*b*	*c*
1	$TiFe_2Sn$	*Fd-3m*	$MnCu_2Al$	0.60601(1) 0.6068 [b]	–	–
2	Ti_5FeSn_3	$P6_3/mcm$	Hf_5CuSn_3	0.8139(5) 0.8152 [b]	–	0.5551(5) 0.5544 [b]
3	$Ti_{0.4}Fe_{0.6}Sn_2$	$P6_222$	Mg_2Ni	0.5496(6) 0.54933 [b]	–	1.3876(6) 1.3845 [b]

[a] Compound number used in the phase diagram (Fig. 1).
[b] Lattice parameters taken from [21-23].
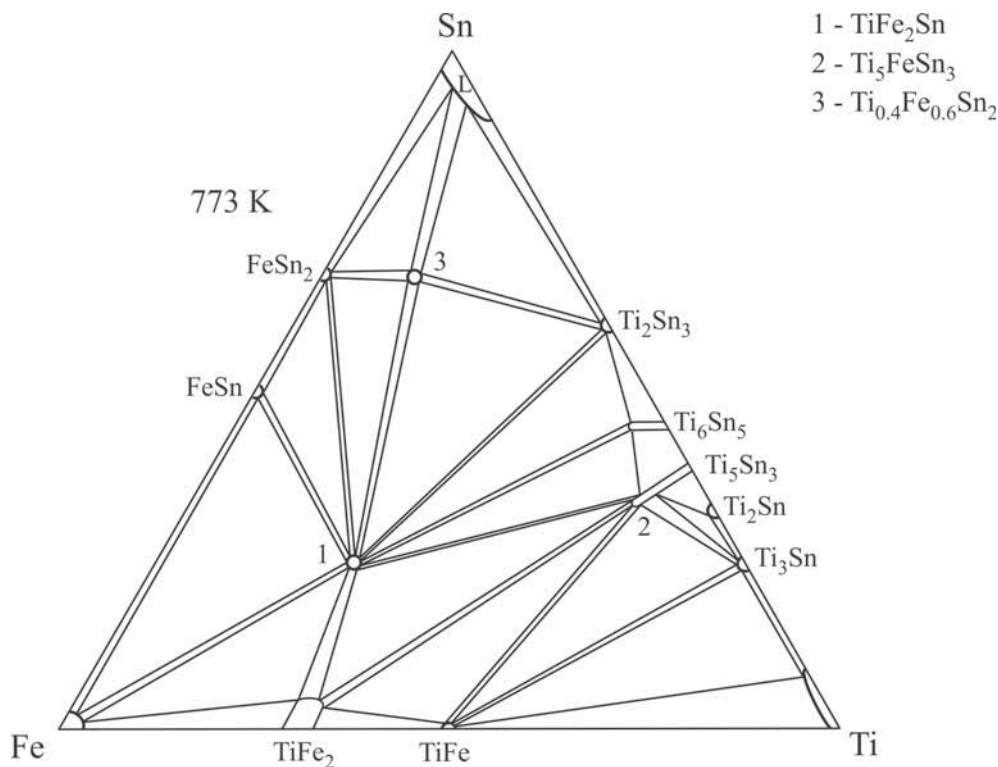
Fig. 1 Isothermal section of the Ti–Fe–Sn phase diagram at 773 K.

The solubility of the third component in the other binary compounds is less than 1-2 at.%.

The phase relations in the Ti–Fe–Sn system are characterized by the formation of three ternary stannides at 773 K (Fig. 1), crystallographic characteristics of which are given in Table 4. The results of EPMA and crystallographic data for selected ternary Ti–Fe–Sn alloys, annealed at 773 K, are presented in Fig. 2 and Table 5.

Equiatomic "TiFeSn" compound?
The TiFeSn compound with MgAgAs-type reported in [24] was not observed during our study of the Ti–Fe–Sn system at 773 K. To check the existence of a TiFeSn stannide at higher temperatures, several samples with compositions close to the stoichiometry 1:1:1 were prepared and annealed at 773, 873, 1073,

and 1173 K. Phase analysis of the corresponding samples at all the investigated temperatures showed the presence of three phases in equilibrium, depending on the small deviation in composition: the main ternary phase $TiFe_2Sn$ and the binaries Ti_6Sn_5 and Ti_2Sn_3, or $TiFe_2Sn$ in equilibrium with Ti_6Sn_5 and Ti_5FeSn_3.

Electronic structure calculations of the TiFeSn compound with lattice parameters taken from [24] and atom distribution like in TiNiSn (Ti (4*a*) 0 0 0; Fe (4*c*) ¼ ¼ ¼; Sn (4*b*) ½ ½ ½) showed that the compound is characterized by positive energy of formation $\Delta E = E_{tot}(TiFeSn) - E_{tot}(hex\text{-}Ti) - E_{tot}(\alpha\text{-}Fe) - E_{tot}(\beta\text{-}Sn) = +7.3$ meV/atom. Optimization of the lattice parameter (Fig. 3) showed that the cell parameter reported in the literature is far from the equilibrated value, 0.633 nm reported in [24]

Table 5 Phase composition and lattice parameters of selected Ti–Fe–Sn alloys annealed at 773 K (in brackets the composition from EPMA data).

| No.	Nominal alloy composition, at.%			Phases		
	Ti	Fe	Sn	1st phase	2nd phase	3rd phase
1	65	28	7	TiFe $a = 0.2973(3)$ nm	Ti$_3$Sn $a = 0.5925(3)$ nm $c = 0.4751(5)$ nm	Ti $a = 0.3157(3)$ nm
2	20	65	15	TiFe$_2$ $a = 0.4800(4)$ nm $c = 0.7831(2)$ nm	TiFe$_2$Sn $a = 0.6061(2)$ nm	Fe $a = 0.2868(2)$ nm
3	35	45	20	TiFe$_2$Sn $a = 0.6062(3)$ nm	TiFe$_2$ $a = 0.4801(3)$ nm $c = 0.7832(1)$ nm	Ti$_5$FeSn$_3$ $a = 0.8137(6)$ nm $c = 0.5540(4)$ nm
4	50	30	20	Ti$_5$FeSn$_3$ (Ti$_{56.17}$Fe$_{10.89}$Sn$_{32.93}$) $a = 0.8135(4)$ nm $c = 0.5545(2)$ nm	TiFe$_2$ (Ti$_{34.49}$Sn$_{65.51}$) $a = 0.4805(4)$ nm $c = 0.7833(3)$ nm	
5	20	50	30	FeSn $a = 0.5286(1)$ nm $c = 0.4436(2)$ nm	TiFe$_2$Sn $a = 0.6060(1)$ nm	
6	30	40	30	TiFe$_2$Sn (Ti$_{26.94}$Fe$_{46.69}$Sn$_{26.37}$) $a = 0.6062(2)$ nm	Ti$_{6-x}$Fe$_x$Sn$_5$ (Ti$_{52.05}$Fe$_{5.35}$Sn$_{42.60}$) $a = 0.9119(4)$ nm $c = 0.5651(2)$ nm	
7	35	25	40	TiFe$_2$Sn $a = 0.6057(3)$ nm	Ti$_{6-x}$Fe$_x$Sn$_5$ (Ti$_{52.05}$Fe$_{5.35}$Sn$_{42.60}$)... $a = 0.9120(2)$ nm $c = 0.5649(2)$ nm	Ti$_2$Sn$_3$ (traces)
8	5	55	40	Ti$_{6-x}$Fe$_x$Sn$_5$ $a = 0.9181(2)$ nm $c = 0.5600(2)$ nm	Ti$_5$Fe$_x$Sn$_3$ $a = 0.8125(3)$ nm $c = 0.5448(2)$ nm	
9	35	20	45	Ti$_2$Sn$_3$ (Ti$_{38.38}$Sn$_{61.25}$) $a = 0.5955(2)$ nm $b = 1.9637(8)$ nm $c = 0.7035(3)$ nm	(Ti,Fe)Sn$_2$ (Ti$_{15.37}$Fe$_{16.42}$Sn$_{68.21}$) $a = 0.5495(2)$ nm $c = 1.3847(2)$ nm	TiFe$_2$Sn (Ti$_{25.42}$Fe$_{46.76}$Sn$_{27.92}$) $a = 0.6061(3)$ nm
10	43	12	45	Ti$_{6-x}$Fe$_x$Sn$_5$ (Ti$_{54.85}$Fe$_{5.45}$Sn$_{39.70}$) $a = 0.9121(3)$ nm $c = 0.5650(1)$ nm	Ti$_2$Sn$_3$ (Ti$_{38.53}$Sn$_{61.47}$) $a = 0.5911(3)$ nm $b = 1.9837(7)$ nm $c = 0.7053(4)$ nm	TiFe$_2$Sn (Ti$_{24.21}$Fe$_{48.84}$Sn$_{26.85}$) $a = 0.6051(3)$ nm
11	10	40	50	FeSn$_2$ $a = 0.6536(4)$ nm $c = 0.5321(2)$ nm	FeSn $a = 0.5285(3)$ nm $c = 0.4469(3)$ nm	TiFe$_2$Sn $a = 0.6035(2)$ nm
12	15	35	50	FeSn$_2$ $a = 0.6538(3)$ nm $c = 0.5324(2)$ nm	TiFe$_2$Sn $a = 0.6035(2)$ nm	Ti$_{0.4}$Fe$_{0.6}$Sn$_2$ $a = 0.5495(6)$ nm $c = 1.3842(9)$ nm
13	20	25	55	Ti$_{0.4}$Fe$_{0.6}$Sn$_2$ (Ti$_{12.56}$Fe$_{19.12}$Sn$_{68.31}$) $a = 0.5500(3)$ nm $c = 1.3850(9)$ nm	TiFe$_2$Sn (Ti$_{25.29}$Fe$_{48.60}$Sn$_{26.11}$) $a = 0.6058(3)$ nm	Ti$_2$Sn$_3$ (Ti$_{39.53}$Sn$_{60.47}$) $a = 0.5912(2)$ nm $b = 1.9836(5)$ nm $c = 0.7051(2)$ nm
14	18	14	68	Ti$_{0.4}$Fe$_{0.6}$Sn$_2$ $a = 0.5503(6)$ nm $c = 1.3848(5)$ nm	Ti$_2$Sn$_3$ $a = 0.5909(1)$ nm $b = 1.9836(6)$ nm $c = 0.7055(5)$ nm	Sn $a = 0.5818(5)$ nm $c = 0.3157(8)$ nm
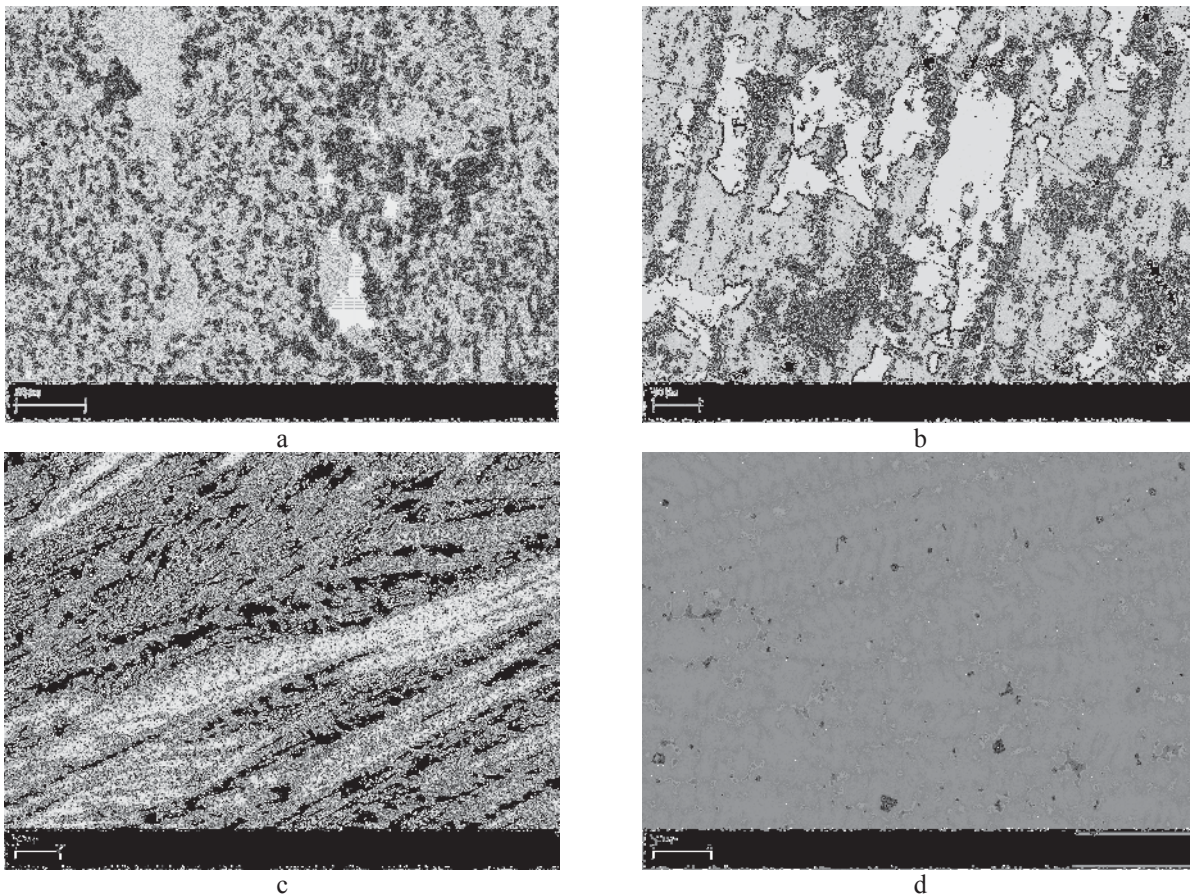
Fig. 2 SEM pictures of alloys from the Ti–Fe–Sn system (the alloys are numbered according to Table 5):
a) 7 – $Ti_{35}Fe_{25}Sn_{40}$: Ti_2Sn_3 (light gray phase), Ti_6Sn_5 (gray phase), $TiFe_2Sn$ (dark gray phase);
b) 9 – $Ti_{35}Fe_{20}Sn_{45}$: $Ti_{6-x}Fe_xSn_5$ (gray phase), Ti_2Sn_3 (light gray phase), $TiFe_2Sn$ (dark gray phase);
c) 4 – $Ti_{50}Fe_{30}Sn_{20}$: $Ti_5Fe_xSn_3$ (gray phase), $TiFe_2$ (dark phase);
d) 6 – $Ti_{30}Fe_{40}Sn_{30}$: $TiFe_2Sn$ (dark gray phase), $Ti_{6-x}Fe_xSn_5$ (gray phase).

compared with a = 0.5816 nm. With the optimized lattice parameters the energy of formation appeared to be negative $\Delta E = -393.3$ meV/atom. Using the phase equilibria from the investigated isothermal section (Fig. 1), we decided to evaluate the energy of the reaction $Ti_6Sn_5+Ti_2Sn_3+8TiFe_2Sn+\Delta H \rightarrow 16TiFeSn$. The values of $\Delta H = +647$ meV/atom for the lattice parameter from [24] and $\Delta H = +249$ meV/atom for the optimized lattice parameter, show that the reaction should run in the opposite direction, confirming the absence of a TiFeSn compound in the Ti−Fe−Sn ternary system.

Ti₅FeₓSn₃ solid solution
The existence of the ternary phase Ti_5FeSn_3 with Hf_5CuSn_3-type [22] was confirmed at 773 K. The Hf_5CuSn_3 structure type (space group $P6_3/mcm$) can be obtained by insertion of Cu atoms into the octahedral voids of the Mn_5Si_3 structure type (two vacancies in the unit cell) [25]. On the other hand, the Hf_5CuSn_3 structure can be considered as a
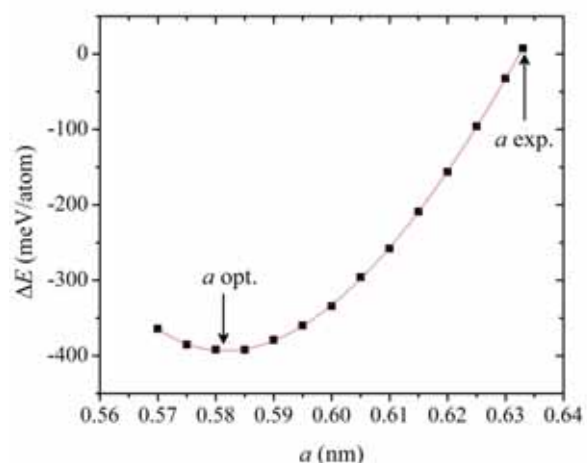

Fig. 3 Optimization of the lattice parameter a for the "TiFeSn" compound; "a opt." corresponds to optimized lattice parameter with the lowest energy and "a exp." to the lattice parameter taken from [24].

Table 6 Lattice parameters of the $Ti_5Fe_xSn_3$ solid solution.

Composition	Lattice parameters, nm		V, nm^3
	a	c	
Ti_5Sn_3	0.8049(2)	0.5454(2)	0.3060(1)
$Ti_5Fe_{0.2}Sn_3$	0.8068(7)	0.5477(7)	0.3087(5)
$Ti_5Fe_{0.4}Sn_3$	0.8083(6)	0.5501(5)	0.3112(4)
$Ti_5Fe_{0.6}Sn_3$	0.8116(5)	0.5522(4)	0.3150(3)
$Ti_5Fe_{0.8}Sn_3$	0.8120(5)	0.5521(4)	0.3152(3)
$Ti_5Fe_{1.0}Sn_3$	0.8139(6)	0.5540(4)	0.3178(4)
$Ti_5Fe_{1.2}Sn_3$ [a]	0.8141(5)	0.5542(4)	0.3180(3)

[a] Two-phase sample.

superstructure of the Ti_5Ga_4 type, which is obtained by inclusion of Ga atoms into the same voids of the Mn_5Si_3 structure type [25]. To verify the process of solid solution formation between Ti_5FeSn_3 (Hf_5CuSn_3-type) and binary Ti_5Sn_3 (Mn_5Si_3-type), additional alloys in the Ti_5Sn_3–Ti_5FeSn_3 region were prepared. The X-ray phase and microprobe analyses of the synthesized samples (Table 6) showed the existence of a $Ti_5Fe_xSn_3$ (x = 0.0-1.0) solid solution formed by insertion of Fe atoms into the octahedral voids (center at position $2b$, 0 0 0) of the Ti_5Sn_3 binary, up to the limiting composition $Ti_{55}Fe_{11}Sn_{34}$ (a = 0.8139(5) nm, c = 0.5551(5) nm). In this reasoning the Ti_5FeSn_3 compound with Hf_5CuSn_3-type corresponds to the extreme composition of the solid solution where Fe atoms have been inserted into binary Ti_5Sn_3 with Mn_5Si_3 structure type.

Electronic structure calculations for the $Ti_{0.4}Fe_{0.6}Sn_2$ compound

The $Ti_{0.4}Fe_{0.6}Sn_2$ compound with Mg_2Ni-type was reported in [23]. During the study of the Ti−Fe−Sn system the presence of the $Ti_{0.4}Fe_{0.6}Sn_2$ compound with $NiMg_2$-type was confirmed at 773 K (the composition according to EPMA data is $Ti_{12.56}Fe_{19.12}Sn_{68.31}$). The authors of [23] analyzed the structural relationship between the $CuAl_2$-type (in our case binary $FeSn_2$ belongs to the $CuAl_2$-type) and the Mg_2Ni-type observed for some ternary phases ($Ti_xV_{1-x}Sn_2$, $Ti_xFe_{1-x}Sn_2$, $V_xFe_{1-x}Sn_2$, *etc.*) and noted the influence of the valence electron concentration and band filling on the stability of these compounds. In our work we performed electronic structure calculations for the $Ti_{0.4}Fe_{0.6}Sn_2$ compound to analyze the chemical bonding in the structure. In order to introduce statistical mixtures, the symmetry of the crystal was reduced and one atom of Ti was substituted for Fe to get the formula $Ti_{0.33}Fe_{0.67}Sn_2$, close to the EPMA data ($Ti_{0.37}Fe_{0.56}Sn_2$). The calculated density of states (Fig. 4) of $Ti_{0.4}Fe_{0.6}Sn_2$ in the paramagnetic state is similar to those of other Mg_2Ni-type compounds reported in [23] and predicts metallic-like behavior. The calculation of the electron localization function (ELF) revealed several features of the structure. The hexagonal nets of Sn1 atoms resemble those in graphite and are characterized by

electron density localization between Sn1 atoms within the hexagonal nets, and between two Sn2 atoms situated above and below the Sn1 hexagonal rings (Fig. 5). The electron density between Ti and Fe is shifted toward the Fe atoms due to the higher electronegativity (χ(Ti) = 1.54, χ(Fe) = 1.83) (Fig. 6). There is also electron density distribution between Sn and Fe atoms. The bonding in the structure can be described in terms of polar intermetallics – the Ti atoms provide electrons to the [FeSn] framework and the excess of Sn atoms allows the formation of Sn-Sn bonds.

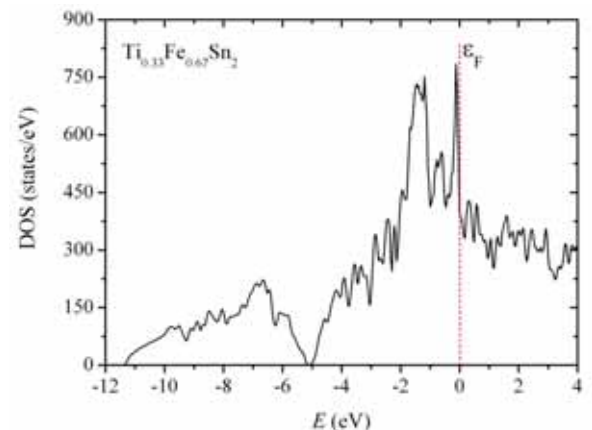**Fig. 4** Distribution of the calculated total density of states of the $Ti_{0.4}Fe_{0.6}Sn_2$ compound.

Final remarks

An analysis of the Ti−Fe−Sn system investigated here and *Me−Me'*−Sn systems studied previously (*Me* = Ti, Zr, Hf; *Me'* = Co, Ni) showed that the Heusler *MeMe'*$_2$Sn compounds with $MnCu_2Al$ structure type are the thermodynamically dominating phases in the systems with Sn [1-4]. The formation of half-Heusler *MeMe'*Sn compounds with MgAgAs-type strongly depends on the electronic configuration of the *d*-metals; the absence of a TiFeSn compound is probably caused by this factor. The *MeMe'*Sn compounds with cubic MgAgAs-type (half-Heusler phases) and *MeMe'*$_2$Sn with cubic $MnCu_2Al$-type (Heusler phases) are characterized by similar
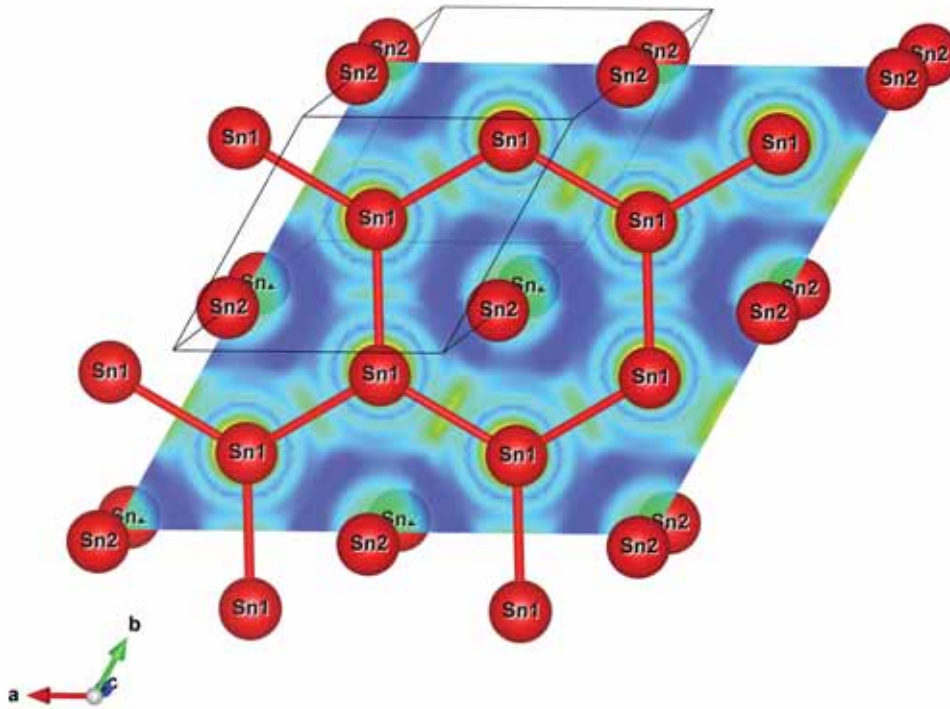
Fig. 5 Projection (at $z = 0.5$) of the electron localization in the range 0.2-0.6 between hexagonal nets of Sn1 atoms and pairs of Sn2 atoms in the $Ti_{0.4}Fe_{0.6}Sn_2$ structure.
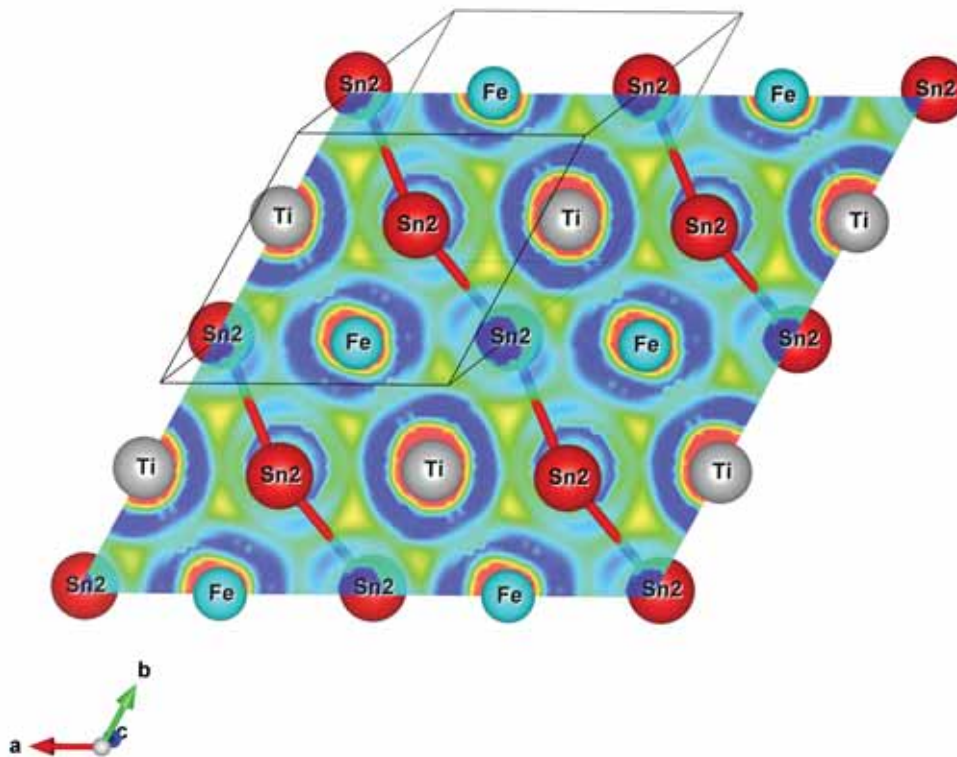

Fig. 6 Projection (at $z = 0.333$) of the electron localization in the range 0.2-0.6 between Ti, Sn and Fe atoms in the $Ti_{0.4}Fe_{0.6}Sn_2$ structure.

crystal structures. The structure of the *MeMe'*$_2$Sn stannides is conventionally presented as a cubic close-packed Sn atomic framework where the octahedral voids are occupied by *Me* atoms and the tetragonal voids are occupied by *Me'* atoms; the *MeMe'*Sn structure can be obtained if one half of the *Me'* atoms are removed so that occupied and unoccupied *Me'* sites are alternating. Despite the similarity of their crystal structures, the *MeMe'*Sn and *MeMe'*$_2$Sn compounds differ by the values of the lattice parameter *a*, normally larger for the completely filled *MeMe'*$_2$Sn phases. Thus, the value reported for TiFeSn (*a* = 0.633 nm) [24], compared with data for TiFe$_2$Sn (*a* = 0.6068 nm) [21], is very surprising. During our study of the Ti–Fe–Sn system the existence of the TiFe$_2$Sn compound with lattice parameter *a* = 0.60601(1) nm was confirmed by X-ray and metallographic analyses, while the TiFeSn phase with *a* = 0.633 nm was not observed under the applied conditions.

Conclusions

The isothermal section of the Ti–Fe–Sn ternary system was constructed at 773 K. At the investigated temperature of annealing three ternary compounds, TiFe$_2$Sn (MnCu$_2$Al-type), Ti$_5$FeSn$_3$ (Hf$_5$CuSn$_3$-type), and Ti$_{0.4}$Fe$_{0.6}$Sn$_2$ (Mg$_2$Ni-type) are formed. The Ti$_5$FeSn$_3$ compound with Hf$_5$CuSn$_3$ structure type is considered to be the limiting composition of an insertion-type solid solution Ti$_5$Fe$_x$Sn$_3$ (*x* = 0.0-1.0), similarly to what has been reported for other *Me–Me'*–Sn systems where *Me* = Ti, Zr, Hf. The compounds with Mg$_2$Ni-type are typical only for the Ti–Fe–Sn (Ti$_{0.4}$Fe$_{0.6}$Sn$_2$), Ti–V–Sn [23] and Ti–Mn–Sn [13] systems. The TiFeSn compound with MgAgAs-type reported earlier was not observed under the applied conditions.

References

[1] Y.V. Stadnyk, L.P. Romaka, V.K. Pecharsky, R.V. Skolozdra, *Neorg. Mater.* 31 (1995) 1422-1425.
[2] L. Romaka, Yu.V. Stadnyk, O.I. Bodak, *J. Alloys Compd.* 317-318 (2001) 347-349.
[3] Yu.V. Stadnyk, R.V. Skolozdra, *Metally* 1 (1994) 164-167.
[4] Yu.V. Stadnyk, L.P. Romaka, *J. Alloys Compd.* 316 (2001) 169-171.
[5] L.P. Romaka, N.O. Koblyuk, Yu.V. Stadnyk, D.P. Frankevych, R.V. Skolozdra, *Pol. J. Chem.* 72(7) (1998) 1154-1159.
[6] Yu. Stadnyk, L. Romaka, A. Horyn, A. Tkachuk, Yu. Gorelenko, P. Rogl, *J. Alloys Compd.* 387 (2005) 251-255.
[7] S.-W. Kim, Y. Kimura, Y. Mishima, *Intermetallics* 15 (2007) 349-356.
[8] D.-Y. Yong, K. Kurosaki, C.-E. Kim, H. Muta, S. Yamanaka, *J. Alloys Compd.* 489 (2010) 328-331.
[9] F.G. Aliev, N.B. Brandt, V.V. Kozyrkov, V.V. Moshchalkov, R.V. Skolozdra, Yu.V. Stadnyk, *Pis'ma Zh. Eksp. Teor. Fiz.* 45(11) (1987) 535-537.
[10] F.G. Aliev, A.I. Belogorohov, N.B. Brandt, V.V. Kozyrkov, R.V. Skolozdra, Yu.V. Stadnyk, *Pis'ma Zh. Eksp. Teor. Fiz.* 47(3) (1988) 151-153.
[11] Yu. Stadnyk, A. Horyn, V.V. Romaka, Yu. Gorelenko, L.P. Romaka, E.K. Hlil, D. Fruchart, *J. Solid State Chem.* 183 (2010) 3023-3028.
[12] N.O. Koblyuk, L.G. Akselrud, R.V. Skolozdra, *Pol. J. Chem.* 73 (1999) 1465-1475.
[13] A.V. Tkachuk, L.G. Akselrud, Yu.V. Stadnyk, O.I. Bodak, *J. Alloys Compd.* 312 (2000) 284-287.
[14] N. Melnychenko-Koblyuk, V.V. Romaka, L. Romaka, Yu. Stadnyk, *Chem. Met. Alloys* 4 (2011) 234-242.
[15] L.G. Akselrud, P.Yu. Zavalii, Yu.N. Grin, V.K. Pecharski, B. Baumgartner, E. Wolfel, *Mater. Sci. Forum* 133 (1993) 335-342.
[16] http://elk.sourceforge.net/
[17] J.P. Perdew, K. Burke, M. Ernzerhof, *Phys. Rev. Lett.* 77 (1996) 3865-3868.
[18] K. Momma, F. Izumi, *J. Appl. Crystallogr.* 41 (2008) 653-658.
[19] T.B. Massalski, *Binary Alloy Phase Diagrams*, ASM International, Metals Park, Ohio, 1990.
[20] H. Kleinke, M. Waldek, P. Gutlich, *Chem. Mater.* 12 (2000) 2219-2224.
[21] Y. Fujita, K. Endo, M. Terada, R. Kimura, *J. Phys. Chem. Solids* 33 (1972) 1443-1446.
[22] J.C. Schuster, M. Naka, T. Shibayanagi, *J. Alloys Compd.* 305 (2000) L1-L3.
[23] U. Häusssermann, S.I. Simak, I.A. Abrikosov, B. Johansson, S. Lidin, *J. Am. Chem. Soc.* 120 (1998) 10136-10146.
[24] R. Kuentzler, R. Clad, G. Schmerber, Y. Dossmann, *J. Magn. Magn. Mater.* 104/107 (1992) 1976-1978.
[25] W. Rieger, H. Nowotny, F. Benesovsky, *Monatsh. Chem.* 96 (1965) 232-241.